

Anatase or Rutile TiO₂ Nanolayer Formation on Ti Substrates by Laser Radiation: Mechanical and Photocatalytic Properties

Arturs Medvids¹, Aleksandrs Michko¹, Aleksejs Jakimovichs¹, Iuriy Naseka²
 Riga Technical University, Paula Valdena 3/7, Riga LV 1048, Latvia¹. E-mail: medvids@latnet.lv
 Institute of Semiconductor Physics, Academy of Science Ukrainian, Kiiv Pr.Nauky 158, Ukraine²

Abstract: A laser-induced oxidation method for the formation of a TiO₂ layer on a Ti substrate was used. The TiO₂ phase can be controlled by an Nd:YAG laser with fundamental frequency at an intensity $I = 52.8 \text{ MW/cm}^2$ and three different doses. Dose $D1 = 3.1 \times 10^{20} \text{ phot/cm}^2$ forms a TiO₂ layer in the anatase phase, which possesses the highest photocatalytic, antibacterial and adhesion properties. As the laser dose increases, the TiO₂ layer thickness increases from 40 nm to 100 nm, but the photocatalytic decomposition reaction constant decreases. The observed super-linear increase of the TiO₂ layer thickness with the laser dose is explained by the presence of positive feedback during the irradiation process. The temperature rises with increasing of the thickness due to the interference-caused decrease of the reflection coefficient. As the thickness increases, TiO₂ on Ti structure adhesion decreases from 800 mN to 400 mN due to the formation of a layer with a mixture of phases.

KEYWORDS: TiO₂ ON TI, RUTILE, ANATASE, LASER RADIATION, PHOTOCATALYLS, HARDNESS

1. Introduction

Titanium (Ti) and its alloys boast excellent properties, including high corrosion resistance and an optimal balance of strength and ductility.

In particular, titanium dioxide in the form of powder or thin coatings has attracted attention in space applications due to its high chemical and radiation resistance, ability to protect surfaces from corrosion and ionizing radiation, as well as photocatalytic properties that can reduce contamination accumulation and improve the durability of materials in outer space conditions [1, 2]. Recently, their use has also been extended to biomedical applications, such as implants, due to their low allergenicity and high compatibility with bone tissue [3, 4]. Titanium (Ti) is coated with a layer of titanium dioxide (TiO₂), and its alloys are increased in corrosion resistance and biocompatibility. Photocatalytic activity is provided, and the material's radiation resistance is increased, which is especially important for use in space conditions [5 - 8]. TiO₂ has various polymorphic phases, including rutile, anatase, and brookite. On the macroscopic scale, rutile is thermodynamically more stable than the other two phases due to its smaller Gibbs free energy [9]. Moreover, an anatase layer on a Ti implant improves its compatibility with bone [5, 6, 10]. Furthermore, anatase and composites of anatase + rutile and anatase + brookite exhibit high levels of photocatalytic activity [11, 12]. Thermal oxidation in a gas atmosphere is a simple and economical method to synthesize a TiO₂ layer on Ti. TiO₂ layers synthesized by thermal oxidation adhere well to Ti substrates. In addition, thermal oxidation can be used for Ti substrates with complex geometries. Many reports have examined the formation of the rutile phase by thermal oxidation of Ti [13].

The anatase phase of TiO₂ is preferable for use in medicine owing to its antibacterial property [3-8]. Additionally, it is the preferred phase for photocatalytic processes such as hydrogen generation at water dissolution [14] and organic molecules disrupting in water or air [15]. On the other hand, TiO₂ in the rutile phase is preferable for use in optoelectronics devices such as UV photodetectors [16] and UV light sources [17]. Such strong application-dependent preferences are due to the different physical properties. First, the band structure is phase dependent. A TiO₂ crystal is an indirect semiconductor in the anatase phase, but it is a direct one in the rutile phase [18]. Therefore, the absorption coefficient of a TiO₂ crystal in the anatase phase is somewhat lower than that in the rutile phase in the range of 3 to 5 eV [19]. Second, the electron lifetime in the anatase phase of a TiO₂ crystal is 100-times higher than that in the rutile phase, which leads to different chemical and biological activities. For example, the anatase phase has better photocatalytic properties than the rutile one. Specifically, the anatase phase has a 100-times larger bipolar diffusion length [18], [20]. Due to the long

lifetime of electrons in the anatase phase (greater than 1 μs), the electron diffusion reaches lengths of more than 10 μm, which are much longer than those in the rutile phase (100 nm) [20].

Claus Hammerl et al. [21] and Elver Juan De Dios Mitma Pillaca et al. [22] used high-fluence oxygen ion implantation to demonstrate the formation of a TiO₂ layer consisting of α-, β-, δ-TiO, rutile TiO₂, and Ti₃O₅ on a Ti substrate. Unfortunately, these methods do not form the anatase phase. Moreover, they cannot control the anatase/rutile phase ratio, which is a very important parameter for photocatalysis, environment purification, etc. To date, laser technology is not often employed in such fine processes as the phase transformation from rutile to anatase [23] or color center formation [24]. One exception is a study where the fourth harmonic of Nd:YAG laser was used for formation of black TiO₂ after irradiating a TiO₂ suspended solution [25]. The XRD patterns suggest that the anatase phase of TiO₂ tends to transform into the rutile phase under a relatively high dose of laser radiation because the rutile phase is more stable at high temperatures and high pressures induced by pulsed laser irradiation. However, an opposite result, where the rutile phase transforms into the anatase one when irradiating a TiO₂ single crystal by a femtosecond Ti cor laser under ablation condition, was reported in [26]. Crystals smaller than 50 nm tend to be in the anatase phase, whereas those larger than 50 nm tend to be in the rutile phase. This phenomenon can be explained by the high pressure produced by a femtosecond laser pulse, although theoretical calculations [9] indicate that the anatase phase is more stable at low pressure. Very often CO₂ laser radiation is used for annealing after TiO₂ layer deposition by the sol-gel method [27] or electron beam evaporation at 200 °C on glass [28]. In these cases, laser radiation is similar to annealing in a furnace. In paper [29], spherical TiO₂ nanoparticles with diameters 4–35 nm were formed by pulsed laser ($\lambda = 1064 \text{ nm}$) ablation of Ti target in water. An advantage of this method is a narrow range of size distribution of nanoparticles, but a disadvantage is their conglomeration. In paper [30], the possibility to transform white TiO₂ to black TiO₂ nanoparticles using Nd:YAG laser radiation ($\lambda = 532 \text{ nm}$) in water was shown. At the same time, the phase transformation from anatase to rutile takes place. Therefore, such a TiO₂ powder can be used in optoelectronics, but, as a photocatalytic, it exhibits low activity [18, 19] due to the decrease of optical band gap and lifetime of electron-hole pairs. Advantages of this method are low cost and limited usage of toxic reagents. In paper [31], photocatalytic water splitting of TiO₂ colloids after an irradiation by nanosecond laser ($\lambda = 532 \text{ nm}$) was studied. It was shown that the efficiency of hydrogen production increases up to a factor of three due to some structural changes in these colloids. This is an unusual effect, since a phase change from anatase towards rutile was also observed, but the efficiency of rutile is known to be

lower than that of the anatase [32]. In paper [33], TiO₂ layer on glass was prepared by spin-coating technique using nanopowder P25. The structure was irradiated by Nd:YAG laser ($\lambda = 266$ nm) at intensity $I = 7.1$ MW/cm² followed by a thermal annealing in air for 1 h at $T = 450^\circ$ C. The irradiation of the structure has led to a transformation of TiO₂ layer from anatase to rutile phase, as in the case of annealing in furnace [34]. As a result of this treatment, the TiO₂ layer became dark. The authors have explained this effect by a decreasing of size of TiO₂ particles. This effect can be more plausibly explained by a surface oxygen depletion, because TiO₂ becomes dark when it is transformed into TiO_x, and the same effect of black TiO_x synthesis in water by a laser-based method was observed in papers [7], [35]. Irradiation of Ti foil by Nd:YAG laser in water [36] leads to formation of a nanoporous black TiO_x. Analysis of surface morphology has shown a certain dependence of surface structure on intensity and number of the pulses. Thus, cracks appeared on the irradiated surface of TiO_x at low intensities and small number of laser pulses, whereas pits were formed at intensities above 300 MW/cm². The specific accumulated fluence for formation of nanopores is about 100 J/cm². The enhancement of the quantum photocatalytic efficiency of TiO_x/Ti/PtNps structure formed by Nd:YAG laser radiation in water is explained as an effect of electron scavenging by the Pt nanoparticles [37]. Advantages of such a technology are its economy, stability, abundance, non-toxicity and high quantum photocatalytic efficiency. In distinction from the reviewed here laser-based methods, we have examined a possibility to form TiO₂ layer on Ti substrate directly by a laser oxidation of Ti plate in air. Because this laser technology is relatively simple, quick, and environmentally friendly, the

formation of TiO₂ by laser oxidation has a great potential for practical applications. The aim of this study is to demonstrate that the phase of TiO₂ layer formed on a Ti substrate by laser oxidation method, can be controlled by irradiation intensity and dose.

2. Experimental

2.1. Laser-induced oxidation method

Prior to the experiments, a pure titanium plate was cut into samples with dimensions about $40.0 \times 15.0 \times 0.3$ mm³. These samples were washed in isopropyl alcohol via an ultrasonic bath and then dried under a dry air flow. TiO₂ thin films on Ti substrates were formed by a laser irradiation method using pulsed Nd:YAG laser radiation ($\lambda = 1064$ nm, pulse duration $\tau = 6$ ns, with $I = 52.8$ MW/cm²). Scanning of the laser beam was performed normally to the Ti surface with the different hatch spacing distances 700 μ m, 550 μ m and 400 μ m resulted in different doses applied on the Ti surfaces: $D1 = 3.1 \times 10^{20}$ phot/cm², $D2 = 3.9 \times 10^{20}$ phot/cm², or $D3 = 5.4 \times 10^{20}$ phot/cm², respectively at constant scanning speeds of the laser ($v = 1$ mm/s). The laser beam diameter was 6 mm. Optical microscope images of TiO₂/Ti structure after irradiation by the laser are shown in Fig.1. Experiments were performed under an atmospheric pressure of 1 atm at 20 °C and 60% humidity. Kinetics of methyl orange photo degradation by TiO₂ formed by laser radiation on Ti substrate with doses D1, D2, D3 are shown in Fig.2.

2.2. Sample characterization

A Raman back scattering spectra identified the phase structure of the TiO₂/Ti samples after laser irradiation with doses D1, D2, and D3 are shown in Fig. 3.



Fig. 1. Optical microscope image of TiO₂/Ti structure after irradiation by the laser doses D1, D2, and D3 at laser intensity 52.8 MW/cm².

Irradiating with doses D1, D2, and D3 form a 40-nm, 70-nm, and 100-nm thick TiO₂ thin film, respectively.

The Raman spectra were measured by a Renishaw InVia90V727 micro-Raman spectrometer with a He-Ne red laser excitation at $\lambda = 633$ nm. The Raman spectra of Ti in the spectral range of 100 cm⁻¹ – 1000 cm⁻¹ after laser irradiation with different doses (Fig. 4) were used for the phase determination.

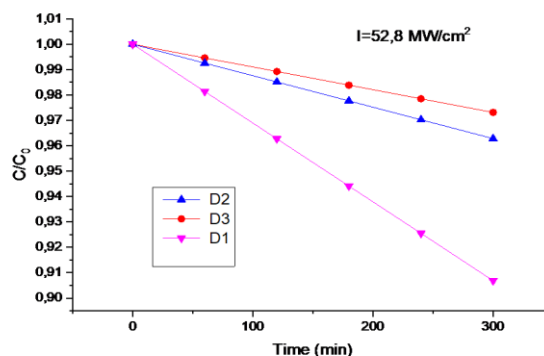


Fig. 2. Kinetics of methyl orange photo degradation by TiO₂ formed by laser radiation on Ti substrate with doses: D1 – pink curve, D2 – blue curve, and D3 – red curve, at laser intensity 52.8 MW/cm². $\alpha_{max} = 3.4 \times 10^{-3} \text{ min}^{-1}$.

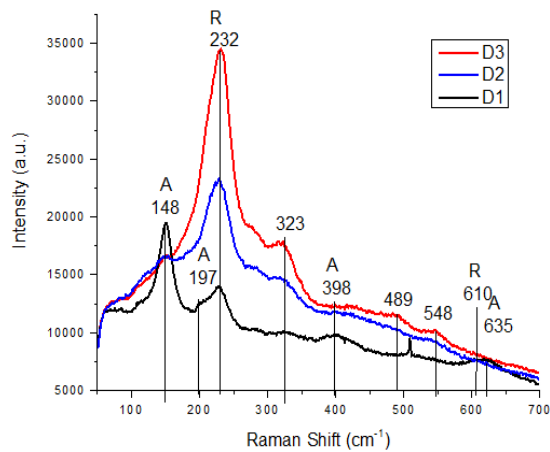


Fig. 3. Raman spectra of TiO₂ thin film on Ti plate formed by the laser radiation with doses D1, D2 and D3.

2.3. Testing of the photocatalytic properties

The photocatalytic TiO₂ layer properties were evaluated by the bleaching of a methylene orange (MO) solution with a concentration of 10 mg/L under UV-A irradiation. Each sample was placed in a beaker and 20 mL of the MO solution was poured over the top. To minimize evaporation, a PS plate was placed on top of the beaker. The samples were then irradiated with a 125-W mercury vapor lamp (365-nm peak wavelength) at a distance of 10 cm. To ensure that the lamp did not heat up the samples, a constant air flow was supplied and the temperature was monitored throughout the experiment. After each hour, 1 mL of the MO solution was extracted to determine the concentration via UV/V is spectroscopy (ThermoScientific, Genesys 10S). After the measurement, the aliquot was returned to the test beaker. Fig. 2 plots the kinetics of MO photodegradation by the samples.

2.4. Scratching method to study TiO₂ on Ti adhesion

The resistance to delamination was investigated by the scratching method (CSM Micro-Combi Tester) using a conical diamond indenter (Rockwell). The scratch force on the scanning indenter was gradually increased from 10 mN to 3.0 N. Fig. 4 shows the critical loads of delamination of TiO₂ thin film on Ti for samples D1, D2 and D3.

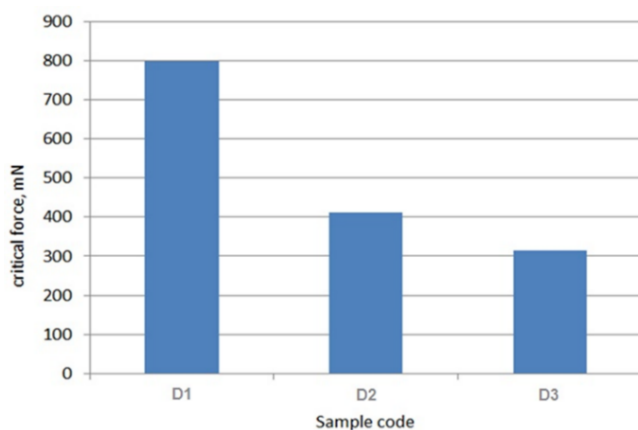


Fig. 4. Critical load of the sample's delamination.

Increasing of the thickness causes a decrease of TiO₂/Ti structure adhesion (critical delamination force) from 800 mN for D1 to 400 mN for D3 due to the formation of a nonhomogeneous TiO₂ layer.

3. Results and discussion

In this study, the impact of the laser radiation on the surface morphology was examined. Irradiating neither does affect the surface smoothness and uniformity nor does form defects or cracks. However, the Ti samples turn dark blue (Fig. 1) after the irradiation by Nd:YAG laser. This change of color is connected to the increased thickness of TiO₂ layer, modifying the picture of interference. Irradiating with doses D1, D2, and D3 form a 40-nm, 70-nm, and 100-nm thick TiO₂ thin film, respectively.

According to the MO bleaching experiment (Fig. 2), the first order reaction constants are $3.2 \times 10^{-4} \text{ min}^{-1}$, $1.1 \times 10^{-4} \text{ min}^{-1}$, and $8.0 \times 10^{-5} \text{ min}^{-1}$ for laser doses D1, D2, and D3, respectively. The D1 dose yields the highest decomposition ratio, while the sample treated using the D3 dose has the lowest decomposition ratio. This can be explained by the decrease in the TiO₂ anatase phase as the laser dose increases.

The analysis of XRD patterns revealed the formation of TiO, Ti₂O₃, anatase TiO₂ and very small amounts of rutile TiO₂ depending on irradiation dose. The most intensive peaks are attributed to Ti, which was observed due to substrate. The most intensive anatase peak is (1 0 1) at 25.3° which was observed after D1 irradiation only. The anatase peak disappeared after irradiation by D2 and D3 doses and peaks of Ti₂O₃ compound became weaker with higher irradiation dose as well. Meanwhile, the intensity of TiO peaks increased with irradiation dose. The simultaneous presence of two phases, as shown in Fig. 3, indicates a TiO₂ heterostructure, having better photocatalytic properties in comparison with the pure anatase or rutile phases, as shown in [11, 12].

The phases change dependence on irradiation dose were evaluated by applying Rietveld deconvolution. The results showed that TiO₂ anatase (which was fixed after D1 irradiation only) constitute about 1.6%. The tendencies showed that the amount of TiO increased from approximately 1.4% to 6.3%, while the amount of Ti₂O₃ compound decreased from approximately 7.3% to 2.8% after the irradiation doses D1 and D3 respectively. The rutile peaks were not included in these calculations due to very weak intensities. The amounts of Ti and O compounds detected are relatively small due to the effect of bulk Ti substrate.

Fig.3 shows the Raman spectra of the three samples after the D1, D2, and D3 doses. The Raman active modes at 148 cm⁻¹, 238 cm⁻¹, 445 cm⁻¹, 610 cm⁻¹, and 829 cm⁻¹ are associated with rutile single crystals, according to [38, 39]. An important property of the anatase and rutile phases in the Raman spectra is the ratio between the band at 148 cm⁻¹ and the band at 610 cm⁻¹. For the anatase phase, the ratio is greater than one, but is less than one for the rutile phase [40]. In our experiments, after the D1 dose, this ratio is ~ 6, suggesting the presence of the anatase phase. However, the Raman spectrum changes after the D2 and D3 doses. The ratio of bands decreases and a new band appears at 232 cm⁻¹, which may be associated with the rutile phase and the increased laser dose. The small regular peaks in regions of 150 cm⁻¹ – 300 cm⁻¹ and 500 cm⁻¹ – 700 cm⁻¹ are related to the disorder induced scattering or second order processes [41].

4. Conclusions

In this paper, the laser oxidation of Ti plate has been investigated. The thickness of TiO₂ layer increases from 40 nm to 100 nm with the laser dose. A positive feedback during the irradiation process is observed: the temperature rises with the increase in the thickness of the TiO₂ layer due to the interference-caused decrease of the reflection coefficient. The thickness of TiO₂/Ti layer rises by increasing the laser irradiation dose from D1 to D3, but adhesion (critical delamination force) of the TiO₂/Ti structure reduces from 800 mN for D1 to 400 mN for D3 due to the formation of a nonhomogeneous TiO₂ layer at doses D2 and D3. This behavior can be explained by mixing of the phases in TiO₂ layer. At D1, the TiO₂ layer is mostly in the anatase phase. However, at D2 and D3, the TiO₂ layer partially transforms into the rutile phase. This

transformation, at least partly, can be explained by the rise of the maximal temperature in the TiO₂ layer at larger doses, as suggested by our calculations, based on the modified Wagner oxidation model. It can be also explained by the deficit of O atoms deeper than 50 nm in Ti substrate at doses D2 and D3 due to the low diffusion of O atoms in Ti.

5. References

- [1] A. Kozlovskiy, M. Zdorovets, *Journal of Nanostructure in Chemistry* (2020) 10(4) pp.331-346.
- [2] E.Deionno, M. Looper, *IEEE Aerospace Conference Proceedings* (2013) pp.15-17.
- [3] P.-I. Brånemark, *J. Prosthet. Dent.*, 50 (3) (1983), pp. 399-410,
- [4] P.I. Brånemark, B.O. Hansson, R. Adell, U. Breine, J. Lindström, O. Hallén, A. Ohman. *Scand. J. Plast. Reconstr. Surg., Suppl.* 16 (1977), pp. 1-132.
- [5] B. Liang, S. Fujibayashi, M. Neo, J. Tamura, H.M. Kim, M. Uchida, T. Kokubo, T. Nakamura, *Biomaterials.*, 24 (27) (2003), pp. 4959-4966.
- [6] C.M. Lin, K. Yen. *Mater. Sci. Eng. C.*, 26 (1) (2006), pp. 54-64.
- [7] X.-F. Yang, Y. Chen, F. Yang, F.-M. He, S.-F. Zhao. *Dent. Mater.*, 25 (4) (2009), pp. 473-480.
- [8] A. Fujishima, T.N. Rao, D.A. Tryk. *J. Photochem. Photobiol. C Photochem. Rev.*, 1 (1) (2000), pp. 1-21.
- [9] D.A.H. Hanaor, C.C. Sorrell. *J. Mater. Sci.*, 46 (4) (2011), pp. 855-874.
- [10] X. Cui, H. Kim, M. Kawashita, L. Wang, T. Xiong, T. Kokubo, T. Nakamura. *Dent. Mater.*, 25 (1) (2009), pp. 80-86.
- [11] T. Kawahara, T. Ozawa, M. Iwasaki, H. Tada, S. Ito. *J. Colloid Interface Sci.*, 267 (2) (2003), pp. 377-381.
- [12] T. Ozawa, M. Iwasaki, H. Tada, T. Akita, K. Tanaka, S. Ito. *J. Colloid Interface Sci.*, 281 (2) (2005), pp. 510-513.
- [13] H. Dong, X.Y. Li. *Mater. Sci. Eng. A* 280 (2000), pp.303-310.
- [14] T. Jafari, E. Moharreri, A. Amin, R. Miao, W. Song, S. Suib. *Molecules.*, 21 (2016), pp. 900-920.
- [15] S. Varnagir, A. Medvids, M. Lelis, D. Milcius, A. Antuzevics. *J. Photochem. Photobiol. A Chem.*, 382 (2019), p. 111941.
- [16] Z.S. Hosseini, M. Shasti, S. Ramezani Sani, A. Mortezaali, J. *Appl. Phys.*, 119 (1) (2016), p. 014503.
- [17] C. Zhu, C. Lv, C. Wang, Y. Sha, D. Li, X. Ma, D. Yang. *Opt. Express.*, 23 (3) (2015), p. 2819.
- [18] T. Luttrell, S. Halpegamage, J. Tao, A. Kramer, E. Sutter, M. Batzill. *Sci. Rep.*, 4 (1) (2015), pp.123-128.
- [19] M.H. Samat, A.M.M. Ali, M.F.M. Taib, O.H. Hassan, M.Z.A. Yahya. *Results Phys.*, 6 (2016), pp. 891-896.
- [20] Y. Yamada, Y. Kanemitsu. *Appl. Phys. Lett.*, 101 (13) (2012), p. 133907.
- [21] C. Hammerl, B. Renner, B. Rauschenbach, W. Assmann. *Nucl. Instruments Methods Phys. Res. Sect. B Beam Interact. with Mater. Atoms.*, 148 (1-4) (1999), pp. 851-857.
- [22] E.J.D.M. Pillaca, M. Ueda, K.G. Kostov, H. Reuther. *Appl. Surf. Sci.*, 258 (24) (2012), pp. 9564-9569.
- [23] E. Dauksta, A. Medvids, P. Onufrijevs, M. Shimomura, Y. Fukuda, K. Murakami. *Curr. Appl. Phys.*, 19 (3) (2019), pp. 351-355.
- [24] J. Chen, L.-B. Lin, F.-Q. Jing. *J. Phys. Chem. Solids.*, 62 (7) (2001), pp. 1257-1262.
- [25] X. Chen, D. Zhao, K. Liu, C. Wang, L. Liu, B. Li, Z. Zhang, D. Shen. *ACS Appl. Mater. Interfaces.*, 7 (29) (2015), pp. 16070-16077.
- [26] H.L. Ma, J.Y. Yang, Y. Dai, Y.B. Zhang, B. Lu, G.H. Ma. *Appl. Surf. Sci.*, 253 (18) (2007), pp. 7497-7500.
- [27] C.-K. Chung, S.L. Lin, K.P. Chuang, S.Y. Cheng, K.Y. Shei. *Micro Nano Lett.*, 7 (8) (2012), pp. 701-705.
- [28] M. Jing, R. Hong, W. Shao, H. Lin, D. Zhang, S. Zhuang, D. Zhang. *Opt. Express.*, 25 (2017), pp. 2377-2382.
- [29] A. Singh, J. Vihinen, E. Frankberg, L. Hyvärinen, M. Honkanen, E. Levänen. *Nanoscale Res. Lett.*, 11 (2016), pp. 1-9.
- [30] V.A. Zuñiga-Ibarra, S. Shaji, B. Krishnan, J. Johny, S. Sharma Kanakillam, D.A. Avellaneda, J.A.A. Martinez, T.K. DasRoy, N.A. Ramos-Delgado. *Appl. Surf. Sci.*, 483 (2019), pp. 156-164.
- [31] S. Filice, G. Compagnini, R. Fiorenza, S. Scirè, L. D'Urso, M.E. Fragalà, P. Russo, E. Fazio, S. Scialese. *J. Colloid Interface Sci.*, 489 (2017), pp. 131-137.
- [32] J. Zhang, P. Zhou, J. Liu, J. Yu. *Phys. Chem. Chem. Phys.*, 16 (38) (2014), pp. 20382-20386.
- [33] M. Sawczak, M. Górski, H. Rachubiński, A. Cenian, *Laser Technol. 2012 Appl. Lasers*. 8703 (2013) 87030M.
- [34] H. Rath, S. Anand, M. Mohapatra, P. Dash, T. Som, U.P. Singh, N.C. Mishra, D. Kanjilal, D.K. Avasthi, S.M. Bose, S.N. Behera, B.K. Roul. *AIP Conf. Proc.*, AIP (2008), pp. 250-255.
- [35] G. Cacciato, M. Zimbone, F. Ruffino, V. Privitera, M.G. Grimaldi. *Phys. Status Solidi Basic Res.*, 254 (7) (2017), p. 1600835.
- [36] G. Cacciato, M. Zimbone, F. Ruffino, V. Privitera, M.G. Grimaldi. *Phys. Status Solidi Basic Res.*, 254 (7) (2017), p. 1600835.
- [37] M. Zimbone, G. Cacciato, R. Sanz, R. Carles, A. Gulino, V. Privitera, M.G. Grimaldi. *Catal. Commun.*, 84 (2016), pp. 11-15.
- [38] S. Mändl, G. Thorwarth, M. Schreck. *Surf. Coatings Technol.*, 125 (2000), pp. 84-88.
- [39] M. Malekshahi, Byranvand, A. Nemat, Kharat, L. Fatholahi, Z. Malekshahi Beiranvand. *J. Nanostructures.*, 3 (2013), pp. 1-9.
- [40] W.F. Zhang, Y.L. He, M.S. Zhang, Z. Yin, Q. Chen. *J. Phys. D Appl. Phys.*, 33 (8) (2000), pp. 912-916.
- [41] H. Schmalzried, A.T. Fromhold, North Holland Publishing Co. 1976. 547 Seiten, *Berichte Der Bunsengesellschaft Für Phys. Chemie*. 81 (1977) 353-354.